

Predicting plasticity of amorphous solids from instantaneous normal modes

Ivan Kriuchevskiy,¹ Timothy W. Sirk,² and Alessio Zaccone^{1,3}

¹*Department of Physics “A. Pontremoli”, University of Milan, via Celoria 16, 20133 Milan, Italy*

²*Polymers Branch, U.S. Army Research Laboratory, Aberdeen Proving Ground, MD, USA*

³*Department of Chemical Engineering and Biotechnology, University of Cambridge, Cambridge CB3 0AS, U.K.*

We present a mathematical description of amorphous solid deformation and plasticity by extending the concept of instantaneous normal modes (INMs) to deformed systems, which allows us to retain the effect of strain on the vibrational density of states (VDOS). Starting from the nonaffine lattice dynamics (NALD) description of elasticity and viscoelasticity of glasses, we formulate the linear response theory up to large deformations by considering the strain-dependent tangent modulus at finite values of shear strain. The (nonaffine) tangent shear modulus is computed from the vibrational density of states (VDOS) of affinely strained configurations at varying strain values. The affine strain, found analytically on the static (undeformed) snapshot of the glass, leads to configurations that are rich of soft low-energy modes as well as unstable modes (negative eigenvalues) that are otherwise completely “washed out” and lost, if one lets the system relax after strain. This procedure is fully consistent with the structure of NALD. The INM spectrum of deformed states allows for the analytical prediction of the stress-strain curve of a model glass, including the prediction of the yield point. Good parameter-free quantitative agreement is shown between the prediction and simulations of athermal quasi-static shear of a coarse-grained polymer glass.

Explaining the emergence of rigidity across the glass transition (T_g) and the fact that the low-frequency shear modulus G goes from zero in the liquid to a finite value in the glassy state is one of the overarching goals of condensed matter physics, with widespread applications from materials engineering [1] to the mechanical stability of amorphous biological matter [2]. An important step towards this goal is to develop a mechanistic understanding of how amorphous solids behave under deformation, i.e. of both their elastic and plastic deformation behaviour. In particular, an understanding of how plastic deformation leads to material yielding and what kind of microstructures promote the plastic flow is currently missing, let alone the possibility of predicting the plastic behaviour in terms of stress vs strain.

While many approaches have aimed at identifying the carriers of plasticity, with moderate success so far given the absence of identifiable microstructures in glass, approaches aiming at describing amorphous plasticity in terms of mechanical instabilities are with no exceptions heavily based on numerical simulations which hinders the mechanistic understanding. In this paper, we tackle this problem from a different angle. By exploiting recent success in mathematically describing the temperature-induced softening and melting of glasses based on the so-called Instantaneous Normal Mode (INM) spectrum [3–6], we apply the same strategy to describe the strain-induced analogues of softening and “melting”, i.e. the plasticity and yielding phenomena [7].

Starting from the seminal work of Squire, Holt and Hoover [8], it became clear that, in the case of amorphous systems (and even complex non-centrosymmetric crystals), in addition to the affine displacements [36], the

mechanical properties are defined by the relaxation of atomic positions towards their equilibrium values, which are called non-affine deformations [9]. These deformations make the material softer, i.e. the elastic shear modulus decreases with increasing non-affinity. It turns out that $G = G_A - G_{NA}$, where G_A is the affine or Born modulus and $-G_{NA}$ is the softening correction from nonaffine displacements [10].

Despite the fact that a formal expression for the non-affine corrections was written early on [8], the concept has been used mainly as a tool to calculate elastic constants in computer simulations [11]. Only recently the mathematical nonaffine response theory of viscoelasticity of amorphous solids was developed [9, 10, 12]. It was again limited to small deformations and *athermal*, meaning that the system resides at, or very close to, a local minimum of the potential energy (inherent state). Further introduction of the so-called instantaneous normal modes (INMs) made it possible to extend the theory to finite temperatures up to the glass transition temperature T_g and slightly beyond [13]. The main idea of INMs is that, instead of characterizing the system in the well-equilibrated inherent states, single snapshots of the non-fully equilibrated system are considered and averaging is performed over the snapshots. This procedure, devised long ago in the context of numerical simulations of liquids [3, 4] (and recently formulated also analytically [6]) allows one to retain crucial information about anharmonicities and saddle-points, which dominate the dynamics of liquids [14] and glasses [15, 16].

The extended theory including INMs (also known as Nonaffine Lattice Dynamics or NALD) yields predictions that agree with coarse-grained molecular dynamics (MD)

simulations [13, 17] and with atomistic simulations [18], quite well without adjustable parameters. In order to compute the viscoelastic moduli of a model glass of N particles with mass m from the MD configurations with the atoms' positions, one needs to know the vibrational density of states (VDOS) $\rho(\omega)$ and the affine force correlator $\Gamma(\omega)$, see Ref.[13] for details. This leads to the following expression for the complex viscoelastic modulus $G^*(\Omega) = G'(\Omega) + iG''(\Omega)$ [9, 13]:

$$G^*(\Omega) = G_A - \frac{3N}{V} \int_C \frac{\rho(\omega)\Gamma(\omega)}{-m\Omega^2 + i\omega\nu + m\omega^2} d\omega. \quad (1)$$

The $\Gamma(\omega)$ can be computed if all the eigenvalues and eigenvectors of the Hessian matrix are known, while the VDOS is just a modified distribution of eigenvalues.

A limitation of the theory presented above is that it works only for small deformations. Upon increasing the shear strain (γ), the amorphous solid can exhibit extensive irreversible plastic deformation. At the moment, there is no way to analytically predict whether a given material state will fail suddenly and catastrophically (brittle failure) or flow like a liquid (ductile yielding). Moreover, we cannot predict when or where it will fail. For disordered solids, including glassy materials, this fundamental question remains a challenge [19–21].

A useful theoretical framework to analyze elementary plastic events is the limit of temperature $T = 0$. To this end, many computational studies on amorphous solids have been performed with the athermal quasi-static (AQS) protocol [22]: a glass sample initially quenched down to zero temperature is deformed by a quasi-static shear procedure consisting of the (nonaffine) relaxation of the system after each strain step. While this protocol still cannot accurately reproduce the elastic and plastic stress-strain response of real materials due to the missing entropic contributions [23–25], it represents a useful framework for developing a deeper physical understanding of plasticity in amorphous solids [26]. As before, the elastic and plastic features of amorphous solids can be understood by analyzing the Hessian matrix [26]. In this case, the NALD equation for the shear modulus reads as [9, 10]

$$G = G_A - \frac{1}{V} \sum_p \frac{\Xi_p^T \cdot \Xi_p}{\omega_p^2}. \quad (2)$$

where ω_p is the p -th eigenfrequency, Ξ_p is the projection of the affine force onto the p -th eigenvector of the Hessian, and V is the volume occupied by the system.

Our aim here is to extend the approach to large deformations and hence to predict the stress-strain curve and the yielding point. We propose to construct the INMs spectrum of deformed states (in short, γ INM) by an instantaneous Affine Transform (AT) from the non-deformed state. This procedure gives us a set of deformed

configurations $\{r(\gamma_i^{AT})\}$. Using these configurations in Eq. 2, we calculate the strain-dependent shear tangent modulus, referred to here as the “local” modulus, from which we predict the stress-strain curve. We will subsequently refer to this procedure as γ NALD. A reconstruction of the whole stress-strain curve of amorphous solids based on modelling the local strain-dependent shear modulus has been presented also in [27], however their continuum model contained a free parameter given by the size of hypothetical Eshelby inclusions, whereas our prediction is entirely parameter-free and from only microscopic quantities.

We also compared the calculations based on γ INM with the calculations obtained with a similar procedure but using, instead of the γ INM states from AT, the fully relaxed states in the local energy minima or inherent states $\{r(\gamma_i^{MIN})\}$. We found that this calculation does not predict any softening nor yielding, but just a steady linear elastic regime, because relaxing the configurations at each strain step effectively washes out all the instabilities, the soft modes, and the saddle-points (see below, in Fig. 1) from the VDOS. This is exactly the same as the case of varying temperature at constant density, where the VDOS of fully relaxed configurations is basically T -independent [13]. Also, if we were to use the energy-minimized configurations after each strain step to compute VDOS and shear modulus with Eq. (1) or Eq. (2), this would lead to an erroneous “double counting” of the nonaffine relaxations. This is because the negative term in Eq. (1) and Eq. (2) already represents the *nonaffine* relaxations from *affine positions* (the Ξ are precisely the force fields that act on the particles in the affine positions [9, 22]), hence it is meaningful and consistent that this term is evaluated using the eigenvalues and VDOS of *affinely* deformed configurations. Finally, we also use the AQS's stress-strain curve as the reference benchmark to test our prediction.

We have used a modified Kremer-Grest model [28] of a coarse-grained polymer system consisting of 100 linear chains of 50 monomers, where the polymer chain consisted of two masses, chosen as $m_1 = 1$ and $m_2 = 3$, placed in an alternating fashion along the chain backbone.

To test the idea described above, a zero temperature configuration of the solid must first be obtained. All of the above quantities can then be extracted from the coordinate snapshots of the system and knowing the interaction potentials. In brief, the snapshots of the system are obtained using the LAMMPS simulation package[29]. After a sufficient number of equilibration steps, the system is slowly quenched below the glass transition temperature T_g , and then the energy minimization is performed. Five replica configurations were constructed, and all results are subsequently averaged over these five glass realizations at $T = 0$.

Each glassy configuration is used as an input for the

calculation of the γ INM. For this we perform an affine transformation (AT) of the initial configuration:

$$\mathbf{r}(\gamma_i^{AT}) = \mathbf{\Lambda} \mathbf{r}(\gamma_0^{AT} = 0) \quad (3)$$

where $\mathbf{\Lambda}$ is the simple shear strain transformation matrix (strain tensor), with all diagonal elements equal to 1, and the only non-zero off-diagonal element $\mathbf{\Lambda}_{xy} = \gamma_i$. The set of γ_i values is chosen such that we do not skip any of the significant plastic events. For every configuration $\{r(\gamma_i^{AT})\}$, we calculate the Hessian matrix H and the affine force field Ξ [9]. The Hessian is then diagonalized to obtain the eigfrequencies ω_p , and the eigenvectors needed to compute the Ξ_p fields projected onto the eigenvectors that enter Eq. (2).

We start by looking at the VDOS of both sets of configurations, $\{r(\gamma_i^{AT})\}$ and $\{r(\gamma_i^{MIN})\}$ (Fig. 1). The VDOS for a polymeric amorphous solid at low temperatures consists of two prominent features: a large peak associated with LJ interactions between beads; and a higher frequency band dominated by FENE bonds vibrations [30]. Also, in the $\{r(\gamma_i^{AT})\}$ configurations, the diagonalization of the Hessian H produces negative eigenvalues and thus imaginary frequencies. The conventional way of depicting these imaginary frequencies is to show their absolute values on the negative part of the frequency axis as discussed many times in the literature [3, 4, 31].

As shown in Fig. 1, the VDOS of the minimized states from AQS, $\{r(\gamma_i^{MIN})\}$, does not show signatures of the deformation, similar to what happens as a function of temperature, where the VDOS of well equilibrated systems barely changes with T . In contrast, the VDOS of affinely strained (i.e. not fully relaxed) states changes significantly, in the same way as the INMs are traditionally extracted from non-fully relaxed MD configurations [3–5]. Moreover, in the γ INM procedure, the increase of γ produces a similar effect on the VDOS, i.e. proliferation of soft low-frequency modes, exactly as for the increase of T on the VDOS of liquids and glasses in standard MD simulations at zero strain (for the latter effect see [5, 13] and references therein). In particular: (i) the population of low-energy and saddle-point unstable (negative eigenvalue) modes increases significantly with increasing strain; (ii) the increase of γ causes the LJ peak and the FENE-bond peaks to decrease and shift to lower frequencies, while a tail of very high-frequency modes emerges at the end of the spectrum and the Debye frequency ω_D is shifted to higher frequencies.[37]

The proliferation of low-energy modes (with positive eigenvalues) directly explains the softening of the material upon increasing γ , similarly to what happens upon increasing T at vanishing strain as shown in [13].

To directly test if the softening predicted by the previous mechanism also occurs in reality, we first semi-analytically calculate the local strain-dependent shear modulus of the $\{r(\gamma_i^{AT})\}$ configurations using Eq. 2. We

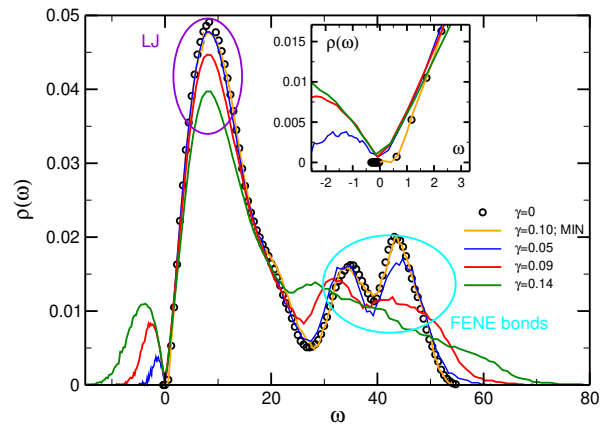


Figure 1: VDOS $\rho(\omega)$ for different affine strains γ_i , showing the INMs spectrum for deformed glasses. Inset gives a closer look at the low- ω region, where we see the increase of the number of low-energy modes with increase of γ . The VDOS for the fully relaxed configuration at $\gamma = 0.1$ from the AQS simulation is also shown, and it basically coincides with the VDOS at $\gamma = 0$ because the energy minimization at each strain step effectively washes out all the soft low-energy modes and the unstable modes.

found that the lowest negative eigenvalue is strongly affected by numerical fluctuations, as reflected in an error bar larger than the mean value [standard deviation of $\mathcal{O}(10^{-2})$ compared with a mean of $\mathcal{O}(10^{-3})$]. Thus, excluding the lowest negative eigenvalue is the most meaningful choice to prevent artifacts caused by large numerical fluctuations. Conversely, for the lowest positive eigenvalue, we consistently observe that its error is much smaller (e.g., the standard deviation never exceeds the mean) hence we retain it in all calculations of the VDOS and subsequently in the stress-strain reconstruction.

Figure 2 shows the local shear modulus as a function of the applied shear strain. For small strains (< 0.05), the shear modulus is relatively stable and stays around $G_0 = 20$, which is the shear modulus of linear elasticity. As we increase γ , the average shear modulus (red curve) decreases, as a manifestation of the strain-induced softening caused by the proliferation of low frequency vibrational modes shown in Fig. 1. Moreover, the shear modulus drops to negative values in a few points, which corresponds to a negative slope in the stress-strain curve or, in another words, to mechanical instabilities (“plastic events”). Already from the behavior of $G(\gamma)$ we can conclude that the largest plastic event occurs at $\gamma \approx 0.1$, which is the typical strain where the yielding of athermal glasses occurs [22].

Using the calculated local shear modulus we then reconstruct the stress via the following algorithm (see also [27]):

$$\sigma(\gamma_i) = \sigma(\gamma_{i-1}) + G(\gamma_i)(\gamma_i - \gamma_{i-1}). \quad (4)$$

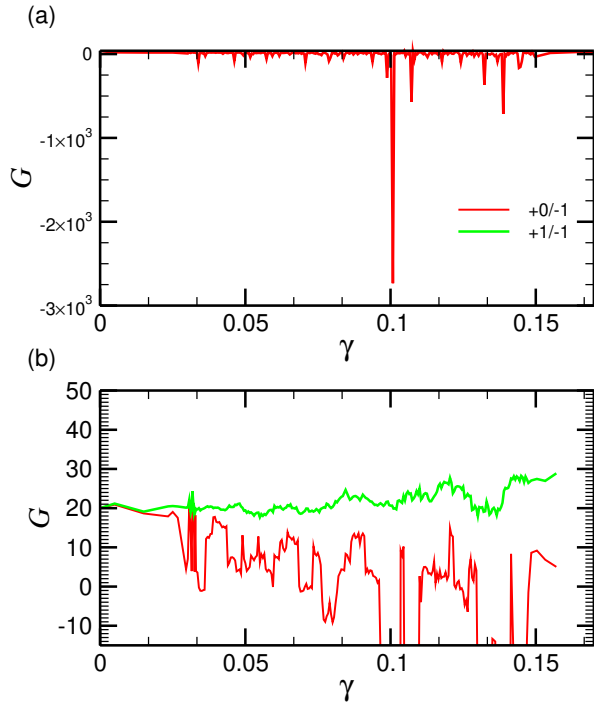


Figure 2: Strain-dependent shear modulus calculated with Eq. 2 using the γ INM spectrum as input. Red - using all eigenvalues except the lowest negative, green - all except the lowest negative and the lowest positive. (b) The running average over 10 points of γ .

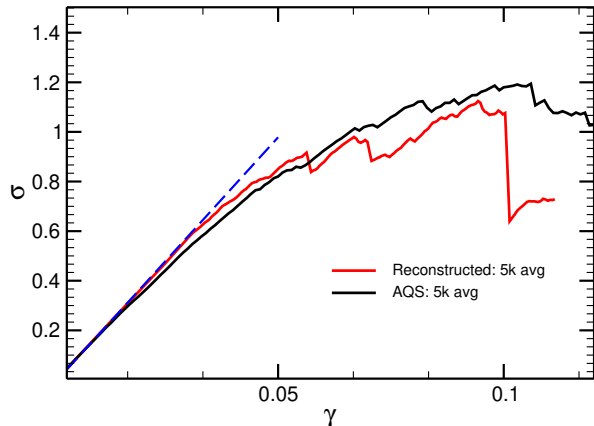


Figure 3: Stress vs strain. Black curve - direct stress recorded along AQS simulation of deformation. Red and Blue curves - stress mathematically predicted from γ NALD (Eq. 2) for the set of snapshots $\{r(\gamma_i^{AT})\}$ of 5k system averaged over 5 replicas.

Figure 2(b) shows the running average of the shear modulus (red) calculated with Eq. 2. If we exclude the lowest positive eigenvalue from the calculation (green), the shear modulus does not significantly change with γ . Moreover it does not become negative at any point. Since the negative G is linked with the plastic events,

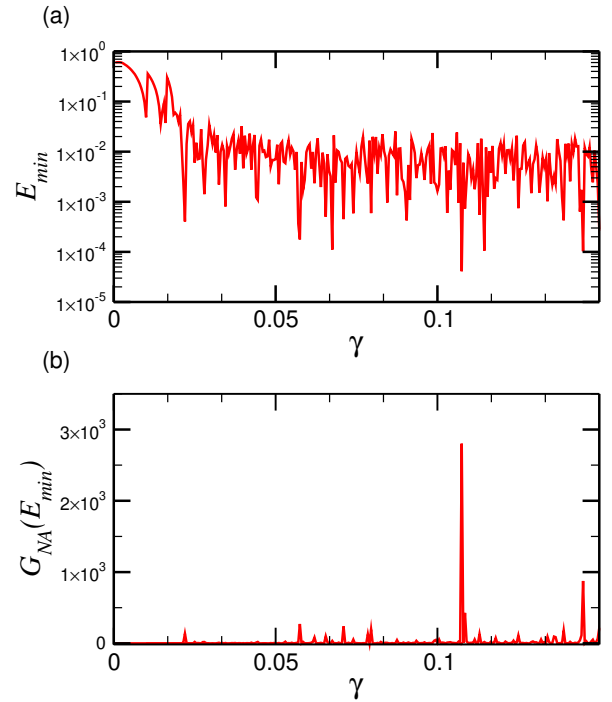


Figure 4: (a) Lowest positive eigenvalue as a function of applied shear strain γ . (b) The contribution of the lowest eigenvalue to the shear modulus G .

this suggests that the lowest positive eigenvalue is primarily responsible for the emergence of plastic events and for the strain-induced softening of the mechanics. In contrast, the role of the unstable modes (i.e., the negative eigenvalues) is to “stabilize” the response, as they correspond mechanistically to the localized nonaffine relaxations (from affine positions) and more extended rearrangements such as avalanches that restore mechanical stability after each AQS deformation step. (Recall that nonaffine relaxations act to restore mechanical equilibrium on the particles by relaxing the affine forces that are present in the affine positions [9, 22]).

We present the stress-strain curves in Fig. 3. Here the black curve corresponds to the stress measured as the direct output of the AQS simulation while the red curve is predicted from the values of $G(\gamma_i)$ computed for the undeformed snapshots, as given in Eq. 4. The semi-analytical calculation (red) gives meaningful results, successfully predicting both the deviation from linearity (blue) at $\approx 5\%$ deformation and the yielding at about 10% strain. Figure 4(a) shows the lowest positive eigenvalue E_{min} for different γ values. On the whole, E_{min} decreases with γ and attains its lowest value around $\gamma = 0.1$, which corresponds to the yielding point. To obtain deeper insight, we consider the contribution of E_{min} to the local shear modulus. Figure 4(b) shows the contribution of E_{min} to the nonaffine term in Eq. 2, which is simply the term with $\omega_p^2 \equiv E_{min}$ in the sum on the r.h.s.

of Eq. 2. As seen in the figure, this serves as an easy way to determine the yield point because of the spectacular sharp peak in this quantity at $\gamma \approx 0.1$. Since $E_{min} > 0$, its contribution to the shear modulus is negative (due to the minus sign in Eq. 2), thus leading to a drop of stress in the stress-strain curve at $\gamma \approx 0.1$. While the connection between the lowest positive eigenvalue and the appearance of plastic events has been highlighted before [32], here we show this in a completely analytical and predictive mathematical framework. One of the main implications of this finding is that one can start with some configurations of the system in the undeformed state, prepare different γ_i states by an analytical affine transformation (AT), and calculate only the lowest positive eigenvalue, which is much faster than calculating the full spectrum, as a function of γ (see Fig. 4): this is enough to predict the yield point of a material without doing any actual simulations of the deformation process.

In summary, we have presented a microscopic mathematical framework that is able to predict, in a parameter free way, the nonlinear deformation and plastic flow transition of amorphous solids. The approach is based on the nonaffine lattice dynamics (NALD) theory of amorphous solids [9, 10, 13, 18] formulated for large strains by extending the concept of Instantaneous Normal Modes to deformed glasses. In this procedure, the mechanical relaxations (and avalanches) are effectively taken into account via the imaginary frequencies (unstable modes) contained in the INMs spectrum of the Affinely Transformed (AT) strained configurations, along with the proliferation of low-energy modes upon increasing strain. These effects can hardly be seen in standard calculations where the energy is minimized after each strain step, whereas in our approach the AT strain, which is the correct input to the nonaffine response calculations, is able to retain all the information about microscopic relaxation processes. Using the INMs of the deformed glass as input to the *nonaffine* shear modulus expression Eq.(2), it is then possible to semi-analytically reconstruct the stress-strain relation in a parameter-free way via Eq. (4). The mathematical prediction, in comparison with actual AQS simulations of the plastic deformation of a coarse-grained polymer glass, is able to capture both the deviation from the linear elastic regime as well as the yielding transition without the need of performing any simulation of the deformation process, i.e. using only MD snapshots of the undeformed material as input. Also, this theory shows that the global yielding transition is strongly driven by the strain-dependent evolution of the lowest positive eigenvalue, which decreases steadily with the applied strain and drives the strain softening process and the yielding. In future work, the spatial structure of this lowest eigenmode may be connected to new topological “defects” that have been recently identified in the displacement field of deformed glasses, and which

can self-organize into a slip system at yielding [33]. The γ NALD approach developed here can be further extended for finite temperatures and for atomistic systems with more complex potentials.

Acknowledgments

A.Z. and I.K. acknowledge financial support from US Army Research Laboratory and US Army Research Office through contract nr. W911NF-19-2-0055.

-
- [1] C. A. Schuh, T. C. Hufnagel, and U. Ramamurty, “Mechanical behavior of amorphous alloys,” *Acta Materialia*, vol. 55, no. 12, pp. 4067–4109, 2007.
 - [2] W. Chen, L. J. Young, M. Lu, A. Zacccone, F. Ströhl, N. Yu, G. S. Kaminski Schierle, and C. F. Kaminski, “Fluorescence self-quenching from reporter dyes informs on the structural properties of amyloid clusters formed in vitro and in cells,” *Nano Letters*, vol. 17, no. 1, pp. 143–149, 2017. PMID: 28073262.
 - [3] T. Keyes, “Instantaneous normal mode approach to liquid state dynamics,” *J. Phys. Chem. A*, vol. 101, no. 16, pp. 2921–2930, 1997.
 - [4] R. Stratt, “The instantaneous normal modes of liquids. accounts of chemical research,” *Macromolecular Theory and Simulations*, vol. 28, no. 5, p. 201–207, 1995.
 - [5] W. Zhang, J. F. Douglas, and F. W. Starr, “What does the instantaneous normal mode spectrum tell us about dynamical heterogeneity in glass-forming fluids?,” *J. Chem. Phys.*, vol. 151, p. 184904, 2019.
 - [6] A. Zacccone and M. Baggioni, “Universal law for the vibrational density of states of liquids,” *Proceedings of the National Academy of Sciences*, vol. 118, no. 5, 2021.
 - [7] D. V. Denisov, M. T. Dang, B. Struth, A. Zacccone, G. H. Wegdam, and P. Schall, “Sharp symmetry-change marks the mechanical failure transition of glasses,” *Scientific Reports*, vol. 5, p. 14359, 2015.
 - [8] D. Squire, A. Holt, and W. Hoover, “Isothermal elastic constants for argon. theory and monte carlo calculations,” *Physica*, vol. 42, no. 3, pp. 388 – 397, 1969.
 - [9] A. Lemaître and C. Maloney, “Sum rules for the quasi-static and visco-elastic response of disordered solids at zero temperature.,” *Physical Review E*, vol. 93, p. 023006, 2016.
 - [10] A. Zacccone and E. Scossa-Romano, “Approximate analytical description of the nonaffine response of amorphous solids,” *Phys. Rev. B*, vol. 83, p. 184205, May 2011.
 - [11] J. F. Lutsko, “Generalized expressions for the calculation of elastic constants by computer simulation,” *Journal of Applied Physics*, vol. 65, no. 8, pp. 2991–2997, 1989.
 - [12] R. Milkus and A. Zacccone, “Atomic-scale origin of dynamic viscoelastic response and creep in disordered solids,” *Phys. Rev. E*, vol. 95, p. 023001, Feb 2017.
 - [13] V. V. Palyulin, C. Ness, R. Milkus, R. M. Elder, T. W. Sirk, and A. Zacccone, “Parameter-free predictions of the viscoelastic response of glassy polymers from non-affine

- lattice dynamics,” *Soft Matter*, vol. 14, pp. 8475–8482, 2018.
- [14] M. Shimada, D. Coslovich, H. Mizuno, and A. Ikeda, “Spatial structure of unstable normal modes in a glass-forming liquid,” *SciPost Phys.*, vol. 10, p. 1, 2021.
- [15] N. Oyama, H. Mizuno, and A. Ikeda, “Instantaneous normal modes reveal structural signatures for the herschel-bulkley rheology in sheared glasses,” 2020.
- [16] V. V. Krishnan, K. Ramola, and S. Karmakar, “Universal non-debye low-frequency vibrations in sheared amorphous solids,” 2021.
- [17] I. Kriuchevskiy, V. V. Palyulin, R. Milkus, R. M. Elder, T. W. Sirk, and A. Zaccone, “Scaling up the lattice dynamics of amorphous materials by orders of magnitude,” *Phys. Rev. B*, vol. 102, p. 024108, Jul 2020.
- [18] R. M. Elder, A. Zaccone, and T. W. Sirk, “Identifying nonaffine softening modes in glassy polymer networks: A pathway to chemical design,” *ACS Macro Letters*, vol. 8, no. 9, pp. 1160–1165, 2019.
- [19] M. L. Falk and J. Langer, “Deformation and failure of amorphous, solidlike materials,” *Annual Review of Condensed Matter Physics*, vol. 2, no. 1, pp. 353–373, 2011.
- [20] A. Nicolas, E. E. Ferrero, K. Martens, and J.-L. Barrat, “Deformation and flow of amorphous solids: Insights from elastoplastic models,” *Rev. Mod. Phys.*, vol. 90, p. 045006, Dec 2018.
- [21] K. L. Galloway, X. Ma, N. C. Keim, D. J. Jerolmack, A. G. Yodh, and P. E. Arratia, “Scaling of relaxation and excess entropy in plastically deformed amorphous solids,” *Proceedings of the National Academy of Sciences*, vol. 117, no. 22, pp. 11887–11893, 2020.
- [22] C. E. Maloney and A. Lemaître, “Amorphous systems in athermal, quasistatic shear,” *Phys. Rev. E*, vol. 74, p. 016118, Jul 2006.
- [23] D. N. Theodorou and U. W. Suter, “Local structure and the mechanism of response to elastic deformation in a glassy polymer,” *Macromolecules*, vol. 19, no. 2, pp. 379–387, 1986.
- [24] P. J. in ’t Veld and G. C. Rutledge, “Temperature-dependent elasticity of a semicrystalline interphase composed of freely rotating chains,” *Macromolecules*, vol. 36, no. 19, pp. 7358–7365, 2003.
- [25] T. W. Sirk, M. Karim, J. L. Lenhart, J. W. Andzelm, and R. Khare, “Bi-modal polymer networks: Viscoelasticity and mechanics from molecular dynamics simulation,” *Polymer*, vol. 90, pp. 178 – 186, 2016.
- [26] D. Richard, M. Ozawa, S. Patinet, E. Stanifer, B. Shang, S. A. Ridout, B. Xu, G. Zhang, P. K. Morse, J.-L. Barrat, L. Berthier, M. L. Falk, P. Guan, A. J. Liu, K. Martens, S. Sastry, D. Vandembroucq, E. Lerner, and M. L. Manning, “Predicting plasticity in disordered solids from structural indicators,” *Phys. Rev. Materials*, vol. 4, p. 113609, Nov 2020.
- [27] T. Albaret, A. Tanguy, F. Boinioli, and D. Rodney, “Mapping between atomistic simulations and eshelby inclusions in the shear deformation of an amorphous silicon model,” *Phys. Rev. E*, vol. 93, p. 053002, May 2016.
- [28] K. Kremer and G. S. Grest, “Molecular dynamics simulation for polymers in the presence of a heat bath,” *Physical Review A*, vol. 33, pp. 3628–3631, 1986.
- [29] P. S, “Fast parallel algorithms for short-range molecular dynamics,” *J Comp Phys*, 1995. See also: <http://lammmps.sandia.gov>.
- [30] R. Milkus, C. Ness, V. V. Palyulin, J. Weber, A. Lapkin, and A. Zaccone, “Interpretation of the vibrational spectra of glassy polymers using coarse-grained simulations,” *Macromolecules*, vol. 51, no. 4, pp. 1559–1572, 2018.
- [31] T. Keyes, “Unstable modes in supercooled and normal liquids: Density of states, energy barriers, and self-diffusion,” *The Journal of Chemical Physics*, vol. 101, no. 6, pp. 5081–5092, 1994.
- [32] R. Dasgupta, S. Karmakar, and I. Procaccia, “Universality of the plastic instability in strained amorphous solids,” *Phys. Rev. Lett.*, vol. 108, p. 075701, Feb 2012.
- [33] M. Baggioli, I. Kriuchevskiy, T. W. Sirk, and A. Zaccone, “Plasticity in amorphous solids is mediated by topological defects in the displacement field,” *arXiv e-prints*, p. arXiv:2101.05529, Jan. 2021.
- [34] K. Kunc, I. Loa, and K. Syassen, “Equation of state and phonon frequency calculations of diamond at high pressures,” *Phys. Rev. B*, vol. 68, p. 094107, Sep 2003.
- [35] C. Setty, M. Baggioli, and A. Zaccone, “Understanding the Effects of Pressure, Anharmonicity and Phonon Softening on the Superconducting Critical Temperature,” *arXiv e-prints*, p. arXiv:2007.04981, July 2020.
- [36] Affine means that the vector distance between two atoms in the deformed solid is given by the vector distance between two atoms prior to deformation left-multiplied by the strain tensor.
- [37] The increase of ω_D with the affine strain can be explained with the fact that, under a simple shear, bonds in the compression sectors of the solid angle are subjected to compression. It is well known that, in solids under pressure, the frequency of optical-like phonons increases with increasing pressure [34], which is important for superconductivity [35].